Astron. Astrophys. 362, 799–808 (2000)

ASTRONOMY AND ASTROPHYSICS

The *Beppo*SAX 2–10 keV survey⋆

P. Giommi[1], **M. Perri**[1], **and F. Fiore**[1,2,3]

[1] BeppoSAX Science Data Center, ASI, Via Corcolle 19, 00131 Roma, Italy
[2] Osservatorio Astronomico di Roma, Via Frascati 33, 00044 Monteporzio, Italy
[3] Harvard-Smithsonian Center for Astrophysics, 60 Garden St., Cambridge, MA 02138, USA

Received 29 March 2000 / Accepted 15 June 2000

Abstract. We present the results of a 2–10 keV *Beppo*SAX survey based on 140 high galactic latitude MECS fields, 12 of which are deep exposures of "blank" parts of the sky. The limiting sensitivity is $5 \times 10^{-14}\ erg\ \mathrm{cm}^{-2}s^{-1}$ where about 25% of the Cosmic X-ray Background (CXB) is resolved into discrete sources. The logN-logS function, built with a statistically complete sample of 177 sources, is steep and in good agreement with the counts derived from ASCA surveys. A CXB fluctuation analysis allowed us to probe the logN-logS down to about $1.5 \times 10^{-14}\ erg\ \mathrm{cm}^{-2}s^{-1}$ where the contribution of discrete sources to the CXB grows to ~ 40–50%.

A hardness ratio analysis reveals the presence of a wide range of spectral shapes and that a fairly large fraction of sources appear to be heavily absorbed, some of which showing soft components.

A comparison of the flux distribution of different subsamples confirms the existence of a spectral hardening with decreasing flux. This effect is probably due to an increasing percentage of absorbed sources at faint fluxes, rather than to a gradual flattening of the spectral slope. Nearly all the sources for which adequate *ROSAT* exposures exist, have been detected in the soft X-rays. This confirms that soft spectral components are present even in strongly absorbed objects, and that a large population of sources undetectable below a few keV does not exist.

A $V_\mathrm{e}/V_\mathrm{a}$ test provides evidence for the presence of cosmological evolution of a magnitude similar to that found in soft X-ray extragalactic sources. Evolution is present both in normal and absorbed sources, with the latter population possibly evolving faster, although this effect could also be the result of complex selection effects.

Key words: surveys – cosmology: observations – X-rays: galaxies – X-rays: general

Send offprint requests to: P. Giommi (giommi@napa.sdc.asi.it)

⋆ Table 1 is only available in electronic form at the CDS via anonymous ftp to cdsarc.u-strasbg.fr (130.79.128.5) or via http://cdsweb.u-strasbg.fr/Abstract.html

1. Introduction

Since the early days of X-ray astronomy many surveys have regularly addressed one of the most intriguing and most intensively studied issues in this field: the nature of the Cosmic X-ray Background (CXB) (e.g. Seward et al. 1967, Boldt et al. 1969, Schwartz et al. 1976, Giacconi et al. 1979, Marshall et al. 1980, Maccacaro et al. 1991, Giommi et al. 1991, Garmire et al. 1992, Hasinger et al. 1993, 1998, McHardy et al. 1998, Zamorani et al. 1999). It is now widely accepted that at least a substantial part of the CXB (above 1 keV) is due to the combined emission of discrete extragalactic sources, mostly AGN, a large fraction of which could be heavily obscured (Setti & Woltjer 1989, Madau, Ghisellini & Fabian 1994, Comastri et al. 1995, Comastri 1999, Fabian 1999, Gilli et al. 1999).

All surveys carried out with the first generation of X-ray telescopes were technically limited to the soft band where photoelectric absorption in the Galaxy, and within the emitters, induces strong biases. As most of the energy of the CXB is instead located in the hard X-rays, despite the very important results obtained with *Einstein* and *ROSAT*, some crucial questions still remain unanswered.

Over the past few years, ASCA and *Beppo*SAX pushed the high energy limit of X-ray optics to about 10 keV removing some of the problems associated to photoelectric absorption. The analysis of ASCA data (Inoue et al. 1996, Georgantopoulos et al. 1997, Cagnoni et al. 1998, Ueda et al. 1998, 1999, Della Ceca et al. 1999a) and the *Beppo*SAX results (Giommi et al. 1998, Giommi et al. 1999a, Fiore et al. 1999, Fiore et al. 2000a) have indeed revealed that absorption plays a crucial role in the making of the CXB and, consequently, that optical surveys might have missed much of the accretion power in the Universe. These findings also showed that the picture is less simple than anticipated due to a) the presence of complex X-ray spectra with soft components even in heavily obscured objects (Giommi et al. 1999a, Della Ceca et al. 1999a), and b) a range of optical properties wider than that found in optical surveys based on color selection. (Schmidt et al. 1998, Fiore et al. 1999, La Franca et al. 2000, Fiore et al. 2000b, Lehmann et al. 2000).

The new generation of powerful X-ray mirrors aboard Chandra and XMM-Newton have already started probing the CXB at very faint fluxes (Brandt et al. 2000, Fiore et al. 2000b,

Mushotzky et al. 2000). Over the next several years these results, together with the outcome of massive optical identification campaigns necessitating the power of the largest existing optical telescopes, will definitively settle many of the open issues. Some issues, however, will probably have to wait for future hard X-ray telescopes operating in the 10–50 keV band, one of the last unexplored energy windows where the bulk of the CXB power is emitted.

In this paper we present the results of a 2–10 keV survey carried out with the MECS instruments aboard *Beppo*SAX (Boella et al. 1997a,b) covering the flux range $\sim 1 \times 10^{-14} - \sim 1 \times 10^{-12}$ erg cm^{-2} s^{-1}. This flux interval is useful to address some of the still open issues, and is helpful for the proper assessment of the bright tail of the much deeper Chandra and XMM-Newton logN-logS. This may be necessary as the determination of the bright part of a logN-logS requires the analysis of large areas of sky. With XMM-Newton or Chandra this can only be achieved by searching for serendipitous sources in a large number of images, many of which will inevitably be centered on targets that may be as bright as the sources sought, lowering the probability of finding other bright serendipitous sources in the same field. This bias also effects the *Beppo*SAX survey but at higher fluxes, above $\sim 1 \times 10^{-12}$ erg cm^{-2} s^{-1}.

The results of a parallel *Beppo*SAX survey, carried out in the harder 5–10 keV band (the HELLAS Survey) are reported in a separate paper (Fiore et al. 2000a). The HELLAS survey was specifically designed to address the issue of hard sources and to take advantage of the MECS PSF, which is sharper in the high energy band.

2. The data

The data used for the survey presented here include 140 MECS fields, 17 of which (12 deep exposures and 5 less exposed) are centered on "blank" parts of the sky. The remaining fields are from observations made as part of one of the main *Beppo*SAX programs, and have been taken from the *Beppo*SAX Science Data Center (SDC) public archive (Giommi & Fiore 1997) after the expiration of the proprietary period. Most of the deep pointings are secondary Narrow Fields Instruments (NFI) observations, that is exposures pointing 90 degrees away from a primary Wide Field Camera (WFC, Jager et al. 1997) target (usually the Galactic Center) and centered on a position chosen to optimize the satellite roll angle. In a few cases the deep exposures were centered near Polaris, the *Beppo*SAX default pointing position in case of safe mode.

The public fields have been selected according to the following criteria:

1. the pointing is at high Galactic latitude ($|b| > 20$)
2. the exposure is longer than 10,000 seconds;
3. the field was public before the end of December 1999;
4. the target of the observation is not too bright (count rate $<$ 0.2 cts s^{-1}) or extended.
5. the field does not include regions such as SMC, LMC, M31, M33 etc..
6. when two fields partially or totally overlap, the one with the deepest exposure is chosen.

The sample so defined covers $\sim$ 45 square degrees of high galactic latitude sky.

Although the number of MECS fields is similar (140) to that of the HELLAS survey (142) the overlap between the two surveys is not very large. This is mainly due to two factors: 1) a relatively large number of fields could not be used in the 2–10 keV band because of condition (4) above, which is necessary to avoid contamination problems connected to the 2–10 keV PSF which is significantly wider than that in the 5–10 keV band, and 2) we include fields that have become public as late as December 1999, whereas the HELLAS survey only uses fields that were public before April 1999. Other differences come from the fact that the 2–10 keV survey must avoid the area obscured by the MECS beryllium support window (which is instead transparent above 5 keV, Boella et al. 1997b) and that the exclusion area around the target is 6 arcminutes radius in the 2–10 keV survey and 4 arcminutes in HELLAS. Finally the useful field of view has been chosen to be 24 arcminutes in the 2–10 keV band and 25 arcminutes in HELLAS.

2.1. Data analysis

The procedure followed for the data analysis is very similar to that used for the *Beppo*SAX HELLAS survey, which is described in detail in Fiore et al. 2000a. We will not repeat all the details here; we will instead summarize the main points and describe the differences with respect to the HELLAS survey.

From the MECS cleaned and calibrated event files we have built X-ray images taking photons with energy channels (PI) between 44 and 220 corresponding to 2–10 keV. Data from all three MECS units were co-added in sky coordinates for observations carried out before the failure of MECS1 on May 7 1997; the sum of MECS2 and MECS3 were used in all other cases. All images have been searched for sources using the detect routine of the XIMAGE package (Giommi et al. 1991) modified as described in Giommi et al. 1998 and in Fiore et al. 2000a. A statistical probability threshold of 5×10^{-4} of being a fluctuation of the local background was chosen so that very few spurious sources should be included in the sample. All the fields centered on "blank" parts of the sky (i.e. not on a previously known X-ray source) were searched over the full field of view (up to an off-axis angle of 24 arcminutes), avoiding the window support structure and two circular regions (8.7 arcmin radius) near the edge of the field of view and centered on the on-board calibration sources. All the observations taken from the public archive have been searched for serendipitous sources outside the central 6 arcminutes to exclude the region immediately surrounding the target of the observation.

Finally each candidate detection has been carefully inspected in various energy bands to remove spurious detections near the edge of the field of view or close to the on-board calibration sources.

2.2. The sky coverage

The sensitivity of the MECS instrument, besides the obvious dependence on exposure time, is a complex and strong function of the position in the field of view. Consequently the area covered by our survey at any given flux (usually known as the sky coverage) is a complex function of flux.

Two basic factors are responsible for this dependence: (1) the effective area decreases at large off-axis angles (vignetting effect) and (2) the Point Spread Function (PSF) degrades with distance from the center. Both these effects depend on energy.

The minimum detectable count rate (cr_{min}) in our MECS images can be analytically described as follows:

$$cr_{min} = cr_o/\sqrt{t}\,(1 + 0.0077R^{1.88}) \quad (1)$$

where cr_o is the minimum source count rate detectable at the center of the field of view, t is the exposure time in seconds, and R is the off-axis radius expressed in arcminutes. The dependence on t is given by $1/\sqrt{t}$ as our X-ray images are always background limited since the minimum exposure time considered is $10,000\,s$. The normalization cr_o has been derived by comparing the predictions of Eq. (1) to the source count rates extracted from our database. We adopted the values $cr_o = 0.24$ and $cr_o = 0.20$ for three and two MECS units respectively. These values are somewhat conservative since some real sources but not necessarily all can still be detected just below the threshold. For the purposes of this paper, however, we prefer to stay somewhat above the ultimate MECS sensitivity limit by rejecting all the sources below the count rate given by Eq. (1). As our simulations show (see Sect. 4) this procedure ensures that a) the number of spurious sources is reduced to a very small percentage; b) the problem of source confusion is minimized; and c) a uniform detection capability over the entire field of view is achieved.

The MECS detectors are very stable, both during single orbits, and over long time periods. The total background level is due to instrumental noise and to the cosmic signal. The first component has been monitored during periods when the sky is occulted by the Earth and has been found to be only slightly decreasing with time with a total change of a few percent since the beginning of the mission. We conclude that, to a good approximation, the values of cr_o can be considered constant throughout the mission.

The sky coverage of our survey has been computed applying the sensitivity law of Eq. (1) to all the 140 MECS fields, taking into account that the areas behind the window support structure and around the calibration sources were not used. Count rates have been converted to 2–10 keV flux assuming a power law spectral model absorbed by an amount of N_H equal to the Galactic value as determined by the 21 cm measurements of Dickey & Lockman (1990). The MECS absolute flux calibration has been checked through several observations of the Crab Nebula carried out at regular intervals throughout the mission. No variations in the MECS sensitivity have been detected (Sacco 1999).

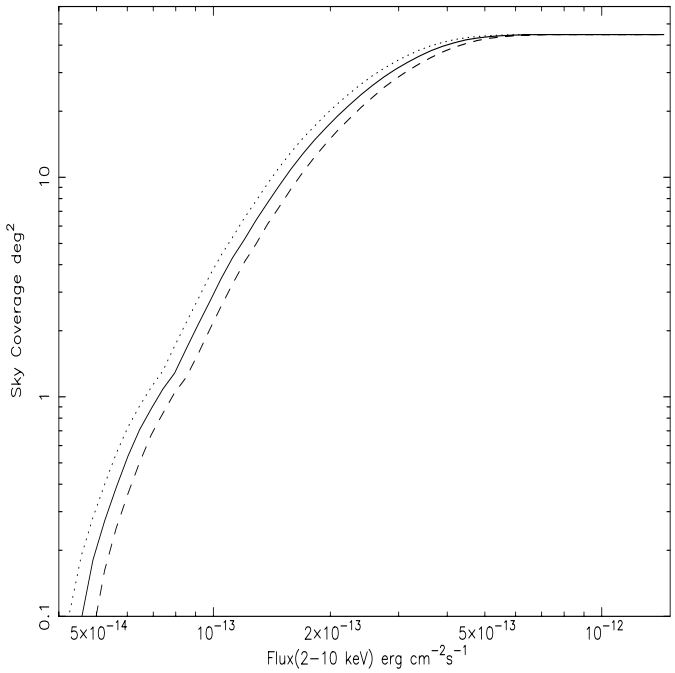

Fig. 1. The sky coverage of the 2–10 keV *Beppo*SAX Survey for three power law energy spectral slopes: $\alpha = 0.2$, dashed line, $\alpha = 0.6$, solid line, and $\alpha = 1.0$, dotted line.

Fig. 1 shows the sky coverage of our survey for three different power law energy slopes, $\alpha = 0.2, 0.6$ and 1.0. Although some dependence on the spectral slope is clearly present, this is not very strong, and the differences are no larger than 20–30% for slopes as different as those considered.

2.3. A statistically well defined sample of 2–10 keV sources

The sources included in our 2–10 keV survey consist of all detections with count rate above the threshold given by Eq. (1). The complete lists, comprising 177 sources, is presented in Table 1 where Column 1 gives the source name; Column 2 gives other designations in case the source was previously known; Columns 3 and 4 give the Right Ascension and Declination; Column 5 gives the 2–10 keV flux calculated assuming a power law spectrum with energy index α = 0.7; Column 6 gives the source classification, and Column 7 give the redshift of extragalactic sources when available.

The uncertainty in the source positions is generally of the order of 1 arcminute, although at large off-axis angles, and in a few cases where some source confusion might be present, this error can be as large as 1.5–2.0 arcminutes (for a more detailed discussion about *Beppo*SAX position uncertainties see Fiore et al. 2000a).

Three quarters of the sources in the list are unidentified. The only identifications are from cross-correlations with catalogs of known objects, the NED and SIMBAD on-line systems, or from the published optical identifications of the HELLAS survey for common sources. The radius used for the correlation is 2 arcminutes; in case the candidate counterpart is found at a

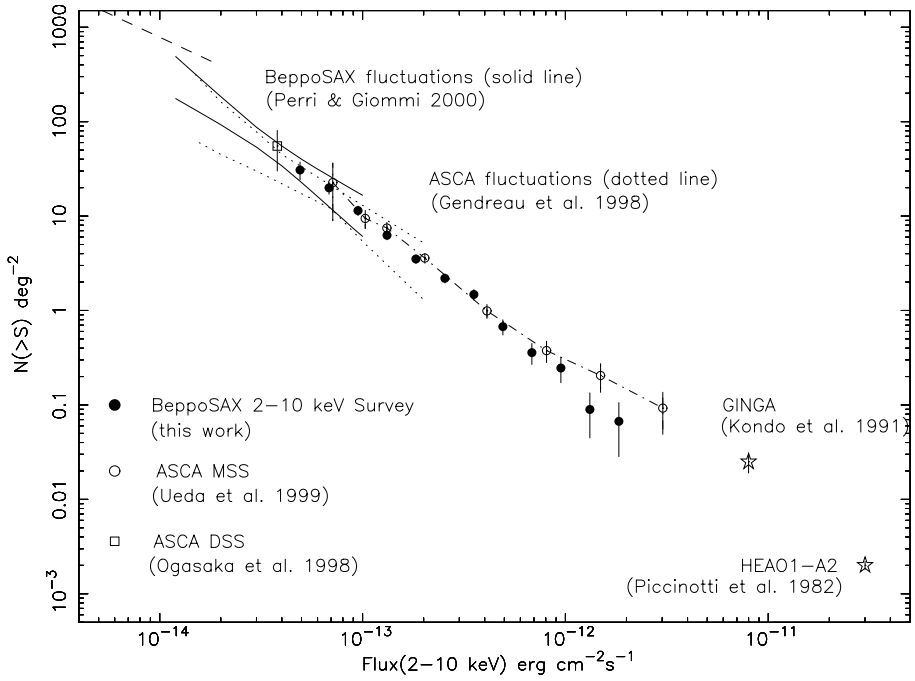

Fig. 2. The 2–10 keV cumulative logN-logS function and the (1 sigma) constraints from the CXB fluctuation analysis derived from *Beppo*SAX and ASCA data. Data points from the ASCA Deep Survey, the ASCA Medium Sensitivity Survey, Ginga and HEAO1-A2 are also shown. The dashed line at the top left indicates the limit obtained imposing that the integrated flux from the discrete sources cannot not exceed 100% of the CXB.

distance larger than 1.2 arcminutes we consider the association as tentative and we add a question mark in Column 2 of Table 1. Of the 45 identified sources, 35 are AGN, 2 are late type stars, one is a RSCVn star system, and 7 are clusters of galaxies. We do not attempt to distinguish between type 1 and type 2 AGN since the identification process is inevitably biased in favor of type 1 AGN which are much better represented in astronomical catalogs than type 2 objects.

From Column 2 in Table 1 we see that 96 *Beppo*SAX sources have soft X-ray counterparts in *Einstein*, *EXOSAT* or *ROSAT* images. Whenever a source in our survey is within one of the *ROSAT* public fields we have checked for possible soft X-ray counterparts. We have found that nearly all *Beppo*SAX 2–10 keV sources are detected also in the 0.2–2.0 keV band if a reasonably deep image exist.

The selection criteria listed in Sect. 2 and Eq. (1) ensure that our sample is statistically well defined and is suitable for statistical analysis.

3. The logN-logS

The X-ray flux distribution of the 177 sources of Table 1 has been combined with the sky coverage of Fig. 1 to estimate the logN-logS function in the 2–10 keV band. The cumulative logN-logS, calculated assuming an average source spectral slope α of 0.7, is plotted in Fig. 2 (filled circles) together with the counts derived from ASCA (open circles) and from other satellites (open stars). The constraints obtained from the *Beppo*SAX CXB fluctuation analysis (see below) are also plotted in the usual "bow tie" shape. Table 2 gives the sky coverage in numerical form together with the cumulative source counts. The *Beppo*SAX logN-logS between 1×10^{-12} and 5×10^{-14} $erg\,\mathrm{cm}^{-2}s^{-1}$ is well described by the relation

Table 2. *Beppo*SAX 2–10 keV Survey Sky Coverage and logN-logS data.

2–10 keV Flux $erg\,\mathrm{cm}^{-2}s^{-1}$	Area deg^2	$N(>S)$ deg^{-2}
4.9×10^{-14}	0.18	30.8 ± 6.6
6.3×10^{-14}	0.65	21.2 ± 3.1
1.0×10^{-13}	2.9	10.3 ± 1.2
1.7×10^{-13}	12.8	4.2 ± 0.4
2.8×10^{-13}	29.6	1.98 ± 0.22
3.5×10^{-13}	36.7	1.48 ± 0.19
5.8×10^{-13}	44.3	0.51 ± 0.11
7.4×10^{-13}	44.7	0.31 ± 0.08
1.2×10^{-12}	44.7	0.089 ± 0.047

$$N(>S) = 10.7 \times (S/10^{-13})^{-1.65\pm0.1} \quad (2)$$

where $N(>S)$ is the number of sources per square degree with flux larger than S in the 2–10 keV band. The best fit values (and 1 sigma error) for the normalization and slope of the logN-logS have been calculated by means of a maximum likelihood method (Murdoch et al. 1973) and are in good agreement with those of ASCA (Della Ceca et al. 1999b).

The logN-logS slope is steeper than the "euclidean value" of 1.5, probably indicating that some amount of cosmological evolution is present.

The agreement with all the ASCA surveys, both in normalization and slope, is very good as can be clearly seen in Fig. 2. The first results on the much deeper Chandra 2–10 keV logN-logS (Mushotsky et al. 2000) is also fully consistent with our data, although the statistics of the Chandra survey in the overlapping flux range is still very limited.

The contribution of the logN-logS sources to the CXB at our flux limit is of the order of 25% (using a CXB intensity of

$2.3 \times 10^{-11}\ erg\,\mathrm{cm}^{-2}\ s^{-1}\ deg^{-2}$ as estimated from *Beppo*SAX MECS data, Vecchi et al. 1999, Perri & Giommi 2000).

4. Simulations and the problem of source confusion

The size of the MECS PSF depends on energy in such a way that the deep exposures in the 2–10 *Beppo*SAX survey are significantly more affected by source confusion then those of the harder (5–10 keV) HELLAS survey. To properly address the effects of source confusion in the *Beppo*SAX 2–10 keV survey we have carried out extensive simulations using the data simulator of the *Beppo*SAX SDC (Giommi & Fiore 1997). A description of this tool can be found at the web page http://www.sdc.asi.it/simulator.

One hundred MECS fields with exposures of 100,000 seconds each were generated and subsequently analyzed following the same procedure used for the survey. Each field included pointlike sources following a logN-logS distribution equal to that measured in the real data above $S = 1 \times 10^{-13} erg\ \mathrm{cm}^{-2} s^{-1}$ and extended down to $S = 1 \times 10^{-14}\ erg\,\mathrm{cm}^{-2} s^{-1}$.

The analysis of these simulated fields resulted in the selection of a large sample of sources that was used to estimate the logN-logS parameters.

Although some cases of source confusion were clearly present no significant bias in the estimation of the logN-logS slope or normalization could be found down to a flux of approximately $5 \times 10^{-14}\ erg\ \mathrm{cm}^{-2} s^{-1}$. At lower flux levels a number of sources could still be detected but in this regime source confusion introduces severe biases in the determination of source flux and accurate positions (see also the results of Hasinger et al. 1998).

In the following we take $5 \times 10^{-14}\ erg\ \mathrm{cm}^{-2} s^{-1}$ as the confusion limit of the MECS instrument.

5. CXB fluctuation analysis

In order to extend our study of the logN-logS relationship beyond the MECS confusion limit of $5 \times 10^{-14}\ erg\ \mathrm{cm}^{-2} s^{-1}$ we have performed an analysis of the spatial fluctuations of the 2–10 keV cosmic background. For reasons of brevity here we only describe the basic steps of the procedure leaving the details to a dedicated paper (Perri & Giommi 2000).

We have used the set of 22 non-overlapping high galactic latitude MECS fields pointed at "blank" parts of the sky which had exposures ranging from 25,000 to 270,000 seconds. To maximize the signal-to-noise ratio and to avoid complications introduced by the MECS window support structure, we have only considered the central 8 arcminutes in each image. Each circular region was then divided in 4 equal quadrants for a total of 88 independent measurements of the CXB.

Net counts were extracted between channel 44 and 200 (2.0–9.0 keV) and converted to flux in the 2–10 keV band assuming a power law spectrum with energy index $\alpha = 0.7$. The MECS internal background (about half of the total signal in the central parts of the field of view) was estimated as in Vecchi et al. (1999) using 3.85 Ms of MECS data accumulated over a period of three years during intervals when the sky was occulted by the Earth. Special attention was used to take into account of instrumental effects such as slight time variations of the MECS internal background and the non-negligible size of the 2–10 keV PSF compared to the regions where the CXB signal was measured.

The observed CXB flux distribution was compared to a number of analytically predicted distributions corresponding to different trial logN-logS parameters. A maximum likelihood test has been used to estimate the best fit and the 68%, ($\Delta S = 2.3$) constraints to the logN-logS slope and normalization which are plotted in Fig. 2 together with the ASCA and *Beppo*SAX logN-logS. A very good agreement is found in the overlapping flux range, whereas the constraints are too weak to detect any slope change just below the ASCA and *Beppo*SAX logN-logS. The additional constraint imposed by the fact that the integrated flux from the logN-logS sources cannot exceed the observed CXB intensity (dashed curve at faint fluxes), however implies that the steep slope measured above $5 \times 10^{-14}\ erg\,\mathrm{cm}^{-2} s^{-1}$ cannot extend much below 2–3 $\times\ 10^{-14}\ erg\ \mathrm{cm}^{-2} s^{-1}$. Similar results at somewhat higher fluxes have been obtained with the analysis of the ASCA fluctuation analysis (Fig. 2 and Gendreau et al. 1998).

Our findings are fully consistent with the first measurements of the 2–10 keV logN-logS at faint fluxes using Chandra data (Mushotzky et al. 2000).

6. Hardness ratio analysis

Earlier *Beppo*SAX results (Giommi et al. 1998, Fiore et al. 2000a) and ASCA surveys (e.g. Ueda et al. 1999, Della Ceca et al. 1999a) convincingly showed that a substantial fraction of serendipitous sources in the 2–10 keV band are either very flat or show evidence for large intrinsic absorption. To test for the presence of hard/absorbed sources in our survey we have carried out a hardness ratio analysis following a procedure that is somewhat different than that of the HELLAS survey.

We have divided the MECS bandpass in three parts: a soft band S (1.3–2.5 keV), a medium band M (2.5–4.4 keV) and a hard band H (4.4–9.6 keV). We have then defined the softness ratio SR=S/M which is sensitive to absorption from $\mathrm{N_H} \sim 1 \times 10^{21}$ up to $\sim 10^{23}\,\mathrm{cm}^{-2}$, and a hardness ratio HR=H/M which is less affected by absorption and allows a better estimation of intrinsic spectral slopes.

Converting the softness ratio into spectral slopes, setting $\mathrm{N_H}$ equal to the Galactic value, we see that there is a very wide range of spectral slopes. In particular, out of the 177 sources in our survey 80 (45%) have a energy slope flatter than 0.5, and about half of these flat sources have negative spectral slopes. This unusual spectral shape is probably not due to extreme spectra (never observed before), but rather the result of intrinsic absorption. In this hypothesis we can quantify the amount of intrinsic $\mathrm{N_H}$ inverting the softness ratios of these sources assuming a spectral index of 0.7. Fig. 3 plots the distribution of the $\mathrm{N_H}$ in excess to

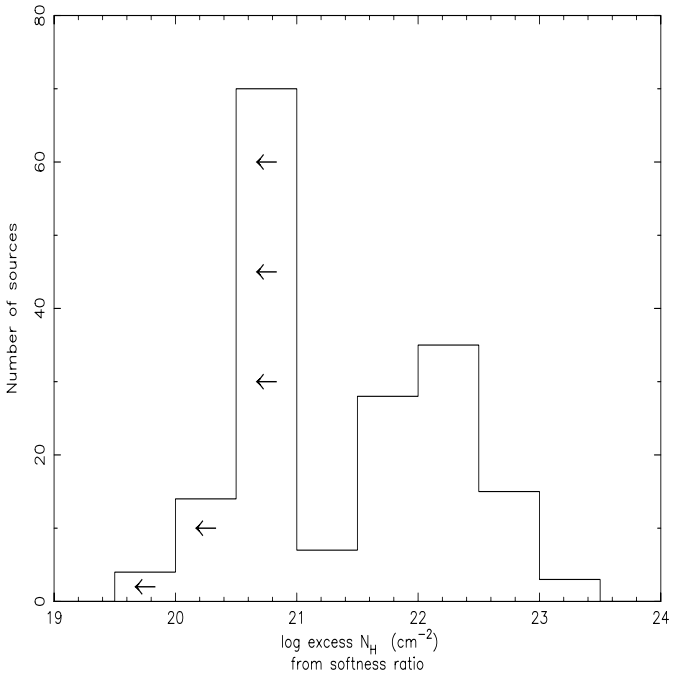

Fig. 3. The distribution of intrinsic N_H and upper limits, as derived from the softness ratio, of the 177 X-ray sources of the *Beppo*SAX 2–10 keV Survey. A power law with energy index $\alpha = 0.7$ was assumed as the underlying spectral model.

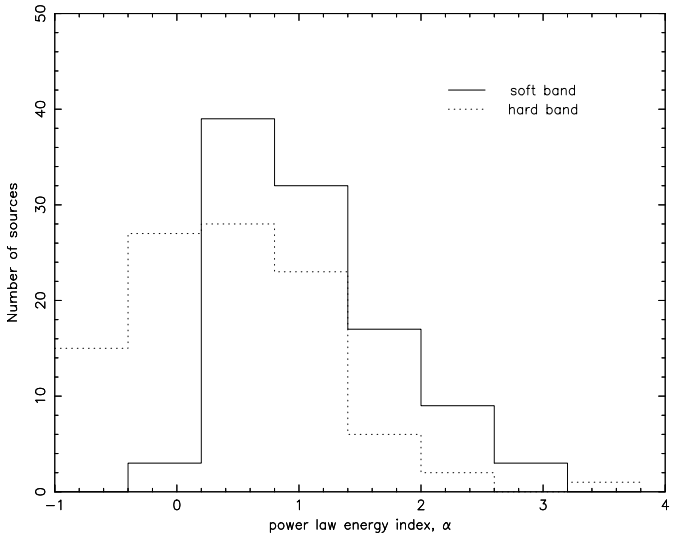

Fig. 4. The distributions of spectral slopes in the soft (1.3–4.4 keV, solid histogram) and hard (2.5–9.6 keV, dotted histogram) band for the 103 sources which are not affected by very large absorption and have been detected with a signal-to-noise ratio larger than 3.5. While there are no very flat slopes in the soft band (because they would have been interpreted as evidence for absorption) a non-negligible fraction of sources in the hard band are very flat ($\alpha_{hard} \lesssim 0$). These spectra could arise from sources where strong absorption is present together with a soft component.

the Galactic value, where it can be seen that intrinsic columns as high as several times 10^{22} cm^{-2} are very common.

We have next considered the subsample of 103 sources detected with a signal to noise ratio (snr) level higher than 3.5 and for which the amount of intrinsic absorption is less than 10^{22} cm^{-2}. We have then calculated the distribution of spectral slopes in the 1.3–4.4 keV band ($\alpha_{\rm soft}$) and in the 2.5–9.6 keV band (α_{hard}) using the softness and hardness ratios respectively. The resulting distributions are plotted in Fig. 4, which shows that the spectral slopes in the hard band appear to be significantly flatter than those in the soft band. The main difference between the two distributions, however, is the presence of a substantial number of very flat slopes in the hard band. Since these sources do not show high intrinsic N_H in the soft band their spectra must be concave (i.e. $\alpha_{\rm soft} > \alpha_{\rm hard}$), as is also apparent from Fig. 5 which plots $\alpha_{\rm hard}$ versus $\alpha_{\rm soft}$ for the subsample of objects detected with a snr larger than 4. These concave spectra could arise from heavily absorbed sources with superposed a soft component. Objects of this type have been found also in ASCA data (Della Ceca et al. 2000). If we assume that all the sources flatter than $\alpha_{hard} = 0.1$ are also absorbed the distributions of $\alpha_{\rm soft}$ and $\alpha_{\rm hard}$ of the remaining sources (i.e. those not showing evidence of absorption, with or without soft component) become very similar ($\langle\alpha_{\rm hard}\rangle = 0.85 \approx \langle\alpha_{\rm soft}\rangle = 0.89$).

To further study the differences between absorbed/unabsorbed and steep/flat sources we have divided our sample into a "steep" (HR$<$ 1.11 90 objects) and a "flat" (HR$>$ 1.11, 87 objects) subsample, and into an "unabsorbed" (SR$>$ 0.55 corresponding to $N_H < 1 \times 10^{22}$ cm^{-2}, 123 objects) and "absorbed" subsample (SR$<$ 0.55, 54 objects). We have then calculated the logN-logS for each subsample after excluding all objects identified with stars or clusters of galaxies. The logN-logS functions of the "absorbed/unabsorbed" subsample are shown in Fig. 6 where it can be seen that the logN-logS of "absorbed" sources (open circles) is significantly steeper than that of the "unabsorbed" sources (filled circles). The logN-logS curves for the "steep" and "flat" subsamples are instead parallel (Fig. 6, top-right) suggesting that the reported spectral differences between bright and faint samples (Ueda et al. 1999, Della Ceca et al. 1999a) are more probably due to a changing percentage of absorbed sources rather than to a change of the intrinsic spectral slope with flux.

This interpretation also explains why the hardening at faint fluxes is not present in the HELLAS survey which was carried out in a band (5- 10 keV) where the effects due to N_H are much less important.

7. Cross-identifications: Soft X-ray counterparts, radio loud sources and blazars candidates

Cross-correlations with catalogs of known soft X-ray sources show that many of the sources in our survey have a soft X-ray counterpart. The correlation with the *ROSAT* WGA catalog (White et al. 1994, Angelini et al. 2000) gives 58 matches within a correlation radius of 1.2 arcmin. We expect that the large majority of these matches are real since repeating the correlation under the same conditions after shifting the coordinates of our sources by a few arcminutes, the number of matches goes down

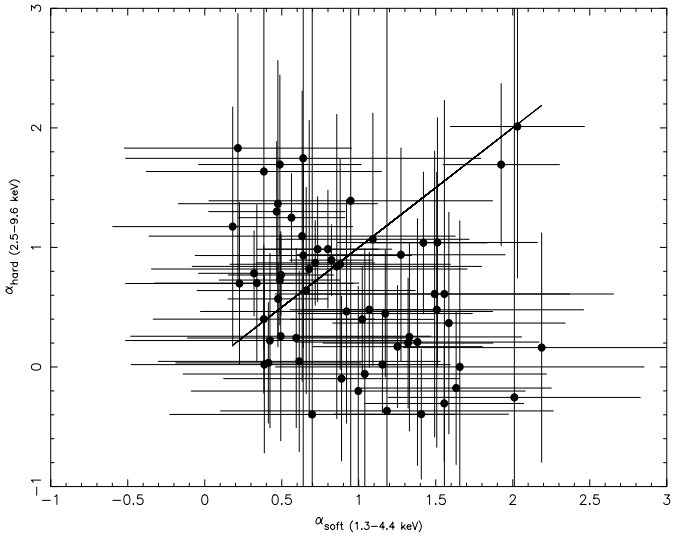

Fig. 5. The power law energy index in the soft (1.3–4.4 keV) is plotted versus the (2.5–9.6 keV) slope for the 62 sources which are not affected by very large absorption and have been detected with a signal-to-noise ratio larger than 4. The solid line marks the $\alpha_{\rm soft} = \alpha_{\rm hard}$ boundary.

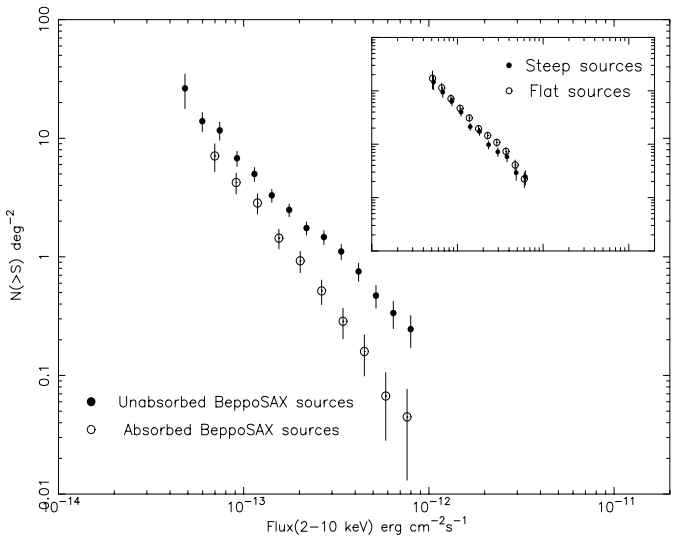

Fig. 6. The 2–10 keV logN-logS for the sub-samples of unabsorbed (filled circles) and absorbed sources (open circles) in the survey. Note that the slopes of the two logN-logS are significantly different; this could be the direct evidence of intrinsically different statistical properties but also the result of complex selection effects (see text). A similar comparison between the sub-samples of flat and steep spectral slope sources (as determined by the hardness ratio analysis in the 2.5–9.6 band) does not show any difference in the logN-logS slope (top-right panel).

to a very small number (1–3, see e.g. Giommi et al. 1999b for an application of this technique). Increasing the correlation radius to 2 arcminutes the number of matches with and without the coordinates shift grows to 77, and to 12–14 respectively, suggesting that about half of the ROSAT/*Beppo*SAX sources between 1.2 and 2 arcminutes are real associations. We have also cross-correlated our catalog with the Rosat All Sky Survey

Table 3. Statistical identification of unidentified sources with radio counterparts.

Name 1SAXJ	NVSS flux (mJy)	m_R^{**}	$\alpha_{\rm ox}$	$\alpha_{\rm ro}$	Tentative identification
0243.1-0023	2.7	18.4	0.99	0.35	HBL BL Lac
0438.7-4727	130*	21.7	0.65	0.88	Blazar
0916.3+2940	25.3	18.7	1.16	0.51	Blazar
1241.5+3251	2.8	18.4	1.1	0.3	HBL BL Lac
1321.7-1635	3.6	19.8	1.01	0.38	HBL BL Lac
1635.5+5955	161	17.5	1.36	0.55	Blazar
2305.9+0902	3.4	16.8	1.47	0.15	Blazar

* 4.85 MHz, from PMN catalog.
** Magnitude estimates are from the USNO catalog.

catalogs RASS-BSC, RASS-FSC (Voges et al. 2000). Whenever a *Beppo*SAX source has a soft X-ray counterpart within 2 arcminutes we report the *ROSAT* (or other satellite) name in Table 1; in case the distance is between 1.2 and 2.0 arcminutes the name of the soft X-ray source is followed by a question mark.

To study the soft X-ray emission of our sources, whenever a *Beppo*SAX object is included in the field of view of one of the PSPC fields available from the *ROSAT* public archive we have visually checked for possible soft X-ray detections. We have found that, with only one exception, all the *Beppo*SAX 2–10 keV sources have counterparts in the 0.2–2.0 keV band, if a reasonably deep image exist (i.e. exposure > 2–$3,000\ s$) and the source is not under the PSPC window support structure. In the only instance where soft X-ray emission was not detected this could either be due to strong variability or to a genuine lack of soft X-ray emission in the cosmic source. Even if the latter is the correct interpretation, we can safely conclude that the percentage of 2–10 keV sources that cannot be detected in the soft X-rays is less than $\sim 5\%$.

A cross correlation of our sample with the the NVSS catalog of radio sources (Condon et al. 1998), and the PMN catalog (Griffith & Wright 1993) for sources south of dec = $-40°$, resulted in 26 matches within a correlation radius =1.2 arcmin. Due to the very large number of faint NVSS sources, however, it is likely that a non-negligible fraction of these matches are accidental. By shifting the coordinates of our sources and rerunning the correlation again we see that the number of spurious associations may be as high as 9-10. To reduce this number to a minimum we have only considered those matches where a) the precise NVSS position coincides with an optical counterpart on the Digitised Sky Survey (DSS) and b) the radio, optical and X-ray flux ratios are within the range seen in previous X-ray surveys.

Assuming that the (only) optical object within the NVSS error region of 1–5 arcsec is the correct counterpart of the *Beppo*SAX source we have derived the broad-band effective spectral indices $\alpha_{\rm ox}$ and $\alpha_{\rm ro}$ (calculated in the rest frame frequencies of 5 GHz, 5000 Å and 1 keV) using the NVSS 1.4 GHz flux (extrapolated to 5.0 GHz), the magnitudes estimates

of the USNO catalog (Monnet 1998) and the *Beppo*SAX fluxes. We have then compared these values to those of known radio sources to check if some of our objects fall in region of the $\alpha_{\rm ox} - \alpha_{\rm ro}$ plane that is typical of Blazars (Giommi et al. 1999a, Perlman et al. 1998). For 13 objects, seven of which previously unknown, this situation is indeed verified. We tentatively identify the latter sources as Blazars and list them in Table 3 where Column 1 gives the source name, Column 2 the NVSS 1.4 GHz radio flux (or the PMN 4.85 GHz flux); Column 3 the m_R from USNO, Columns 4 and 5 give the $\alpha_{\rm ox}$ and $\alpha_{\rm ro}$, and Column 6 gives a tentative identification based on the $\alpha_{\rm ox}$ and $\alpha_{\rm ro}$ values as in Giommi et al. (1999).

Table 4. $V_{\rm e}/V_{\rm a}$ results, full survey (excluding stars and clusters of galaxies), 167 sources

Assumed redshift	$\langle V_{\rm e}/V_{\rm a}\rangle$
0.2	0.607± 0.022
0.5	0.649± 0.022
1.0	0.685± 0.022
MC z distribution [a]	0.643 ± 0.022 [b]
	[0.637–0.650] [c]

[a] Monte Carlo simulated redshifts based on the redshift distribution of the presently identified sources in the ASCA LSS survey.
[b] Average value of $\langle V_{\rm e}/V_{\rm a}\rangle$ with Monte Carlo simulated redshifts.
[c] 90% range of $\langle V_{\rm e}/V_{\rm a}\rangle$ in 100 simulation runs.

8. The $V_{\rm e}/V_{\rm a}$ statistics and cosmological evolution

The $V/V_{\rm m}$ statistics (Schmidt 1968), and its extension $V_{\rm e}/V_{\rm a}$ (Avni & Bachall 1980) to surveys with many flux limits like the *Beppo*SAX 2–10 keV survey, provides an effective and model-independent way to test for the presence of cosmological evolution. Due to the relativistic geometry of the Universe and to the K-correction, the $V_{\rm e}/V_{\rm a}$ value depends on redshift, a quantity that is not known for the large majority of our sources. We have nevertheless applied the $V_{\rm e}/V_{\rm a}$ test (in the framework of a Friedmann cosmology with $q_0 = 0$) assuming a range of redshift values for all unidentified sources. Table 4 summarizes the results. Column 1 gives the assumed redshift, Column 2 gives the $\langle V_{\rm e}/V_{\rm a}\rangle$ with its 1 sigma statistical uncertainty given by $\sqrt{(12N)}$, where N is the number of sources. For all values of the assumed redshift the $\langle V_{\rm e}/V_{\rm a}\rangle$ is significantly higher than 0.5, the expected value for a population of non-evolving objects. Even in the most conservative case where redshift of unidentified objects is fixed to 0.2, the $\langle V_{\rm e}/V_{\rm a}\rangle$ is about five sigma higher than 0.5 rejecting the hypothesis of a uniform distribution with a confidence higher than 99.99%. This case is almost certainly too conservative, since the redshift distribution of the sources so far identified in the HELLAS and ASCA surveys reaches values well in excess 0.2 (Akiyama et al. 2000, La Franca et al. 2000). If instead of using a single fixed redshift value we use Monte Carlo simulated redshifts, generated from the redshift distribution of the ASCA MSS survey (Akiyama et al. 2000), we find a mean value of $\langle V_{\rm e}/V_{\rm a}\rangle$ of 0.643 and a 90% range of 0.637 and 0.650 in 100 simulation runs. We conclude that, despite the limited knowledge of the redshifts of our sources, the $V_{\rm e}/V_{\rm a}$ test provides strong evidence for the presence of substantial cosmological evolution in the *Beppo*SAX 2–10 keV survey.

Assuming a pure luminosity evolution law of the form $L(z) = L(z = 0) \times (1 + z)^C$ and the redshift distribution simulated as described above, we can quantify the amount of cosmological evolution present in our sample. We do that calculating $V_{\rm e}/V_{\rm a}$ varying the value of the evolution parameter C until the $\langle V_{\rm e}/V_{\rm a}\rangle$ is 0.5 (or 0.5 plus or minus the statistical error). This method gives $C = 2.35 \pm 0.2$, a value that is very close to those of $C = 2.5$–2.7 derived in soft X-ray surveys (Maccacaro et al. 1991, Boyle et al. 1994, Page et al. 1996) and in combinations of ROSAT and ASCA data (Boyle et al. 1998). Given the limitations of our sample we do not attempt to fit more complex evolution laws (Miyaji et al. 2000).

As in Sect. 6 we have also divided our sample in two parts: a) sources with high intrinsic absorption ($\rm N_H > 1 \times 10^{22}\,cm^{-2}$) and b) sources with no evidence for high intrinsic absorption. The $\langle V_{\rm e}/V_{\rm a}\rangle$ for the two subsamples are listed in Table 5 were it can be seen that in both cases they are significantly higher than 0.5 and that the value of $\langle V_{\rm e}/V_{\rm a}\rangle$ for the sample of absorbed sources is somewhat higher than that of the unabsorbed ones for all value of the assumed redshifts. The evolution parameter C, derived using the proper ASCA redshift distributions for absorbed and unabsorbed objects, (taken from Akiyama et al. 2000) is $C = 3.0 \pm 0.4$ and $C = 2.1 \pm 0.3$ respectively, indicating that a substantial amount of cosmological evolution is present in both subsamples and that this is possibly higher in absorbed sources. This different evolution rate in absorbed sources, however, could also be induced by complex selection effects since the conversion between count rate and flux (which depends on the amount of intrinsic absorption, the average luminosity and redshift) is most probably a function of intensity, rather than a constant value as we have assumed.

9. Summary and conclusions

We have selected a statistically well defined sample of 177 hard X-ray sources discovered in 140 *Beppo*SAX MECS fields covering ~ 45 square degrees of high galactic latitude sky. About 25% of the sources have been identified through cross-correlations with astronomical catalogs or using NED or the SIMBAD online systems; 96 sources have also been detected in soft X-ray images.

The 2–10 keV logN-logS in the flux range $5 \times 10^{-14} - 2 \times 10^{-12}$ erg cm^{-2} s^{-1} is steeper than that expected for a population of non-evolving sources in an euclidean universe. The best fit to the cumulative distribution is $N(> S) = 10.7 \times (S/10^{-13})^{-1.65\pm0.1}$ and is in good agreement with the counts derived from various ASCA surveys (Cagnoni et al. 1998, Ueda et al. 1998, 1999, Della Ceca et al. 1999a).

A CXB fluctuation analysis, performed on 22 fields centered on random parts of the sky, allowed us to constrain the logN-logS relationship down to about 1×10^{-14} erg cm^{-2} s^{-1}. The first

Table 5. $V_{\rm e}/V_{\rm a}$ results, comparison between samples of absorbed and unabsorbed objects

Sample	Number of objects	Assumed redshift	$\langle V_{\rm e}/V_{\rm a}\rangle$
Absorbed	51	0.2	0.656± 0.040
sources	51	0.5	0.698± 0.040
	51	1.0	0.734± 0.040
	51	MC [a]	0.656 ± 0.040 [b]
			[0.645–0.666] [c]
Unabsorbed	116	0.2	0.585± 0.027
sources	116	0.5	0.624± 0.027
	116	1.0	0.658± 0.027
	116	MC [d]	0.629 ± 0.027 [b]
			[0.620–0.636] [c]

[a] Monte Carlo simulated redshifts based on the redshift distribution of the presently identified absorbed sources in the ASCA LSS survey.
[b] Average value of $\langle V_{\rm e}/V_{\rm a}\rangle$ with Monte Carlo simulated redshifts.
[c] 90% range of $\langle V_{\rm e}/V_{\rm a}\rangle$ in 100 simulation runs.
[d] Monte Carlo simulated redshifts based on the redshift distribution of the presently identified unabsorbed sources in the ASCA LSS survey.

estimate of the faint 2–10 keV Chandra logN-logS (Mushotzsky et al. 2000) is fully consistent with our results.

The hardness ratio analysis reveals that a good fraction of 2–10 keV sources in the flux interval covered by our survey are intrinsically absorbed (Fig. 3). Figs. 4 and 5 show that the range of spectral slopes is very wide and that some objects are characterized by extremely flat (sometimes negative) slopes in the hard band but do not appear to be absorbed or flat in the soft band. This result is in line with the findings of Giommi et al. 1999 who reported that the spectrum of extragalactic X-ray sources must include a soft component even in heavily cutoff objects, thus explaining why nearly all our 2–10 keV sources are also detected in soft X-ray images. Similar conclusions have been drawn from ASCA data by e.g. Della Ceca et al. (2000). One possibility is that these complex spectra could arise from regions producing both an absorbed and an unabsorbed component ("leaky absorber") with the latter originating from scattering by warm material above the absorbing torus, or from partial covering. Another possibility is that the unabsorbed component comes from circumnuclear starburst regions or winds.

Dividing our sources into different subsamples we showed that the logN-logS of absorbed sources is steeper than that of unobscured objects. This trend is foreseen by CXB synthesis models and our findings are in broad agreement with the predictions of the models described in e.g. Comastri 1999.

A $V_{\rm e}/V_{\rm a}$ test provides strong evidence for the presence of substantial cosmological evolution for any reasonable assumption on the redshift of our unidentified sources. Assuming Monte-Carlo simulated redshifts drawn from the observed distributions in the ASCA surveys, and a luminosity evolution law of the form $L(z) = L(z = 0) \times (1 + z)^C$, we have been able to quantify the amount of cosmological evolution present in our survey. The evolution parameter C is estimated to be in the range C=2.1–2.5, a value that is similar to that found in soft X-ray surveys (Page et al. 1996, Boyle et al. 1994, 1998). Evolution is present in both unobscured (C=1.8–2.4) and absorbed sources (C=2.6–3.4) with the latter population possibly evolving faster. We note however that this difference could also be due to observational biases arising from possible correlations between physical or geometrical parameters such as luminosity, $N_{\rm H}$ etc.., or simply due to an intensity dependent count rate-flux conversion factor, rather than to a different rate of evolution of the central engine in absorbed and unabsorbed sources. Indeed CXB synthesis models predict an increasing percentage of absorbed sources at faint fluxes even assuming the same rate of cosmological evolution for all AGN (Comastri et al. 1999, Gilli et al. 1999).

Since cosmological evolution is one of the key ingredients in CXB models, confirmation (and a more precise assessment) of this result would have important implications for the understanding of the CXB.

We find that 13 objects are associated to radio-loud sources. A statistical identification technique, based on their location in the $\alpha_{\rm ox} - \alpha_{\rm ro}$ plane, allowed us to preliminarily identify 7 sources with blazars, some of which are probably high energy peaked (HBL) BL Lacs. This number is consistent with the expectations from the logN-logS of BL Lacs in the soft X-rays (Wolter et al. 1991, Padovani & Giommi 1995).

Nearly all the *Beppo*SAX 2–10 keV sources within the field of view of one of the *ROSAT* images have a soft X-ray counterpart. This implies that if a population of 2–10 keV sources that are undetectable in the soft band exist, it must be a very small percentage of the total. Such a population was put forward as a possible explanation for the normalization of the 2–10 keV Ginga logN-logS (as derived from a fluctuation analysis) which was a factor 2–3 higher than the extrapolation of the 0.3–3.5 *Einstein* logN-logS assuming the canonical power law (energy) spectral slope of 0.7 (Butcher et al. 1997). Our findings (see also Fiore et al. 2000a), and those of ASCA, clearly show that the situation is more complex and rather different from the first simple interpretation of the CXB as the superposition of AGN with a "canonical" power law spectral slope of 0.7 which gave rise to the "spectral paradox".

CXB synthesis models went a significant step further incorporating into the picture the unified schemes for AGN and a number of parameters to describe the luminosity functions of absorbed and unabsorbed sources and their cosmological evolution. The *Beppo*SAX and ASCA results are contributing to provide constraints to the parameters space and to reveal new phenomena. Chandra and XMM-Newton will undoubtly significantly improve our understanding of the CXB. However, the sensitivity has now gone past the point where different components (originating in the central engine, from partial covering, through reflections, and from starburst activity or from other circumnuclear sources) mix together causing severe complications to the interpretation of the data. A complete understanding of the CXB will probably have to wait for future X-ray missions operating well above 10 keV providing for the first time an unobstructed view of the central engine of the sources making what was known as the diffuse background.

Acknowledgements. We thank F. Tamburelli for her crucial contribution to the upgrading of the XIMAGE detect routine, M. Capalbi for her help with the *Beppo*SAX archive, and A. Matteuzzi for his hard work on the MECS data reduction software. We wish to thank R. Della Ceca for running the Brera Observatory Maximum Likelihood code on our logN-logS data and Y. Ueda for providing us with the AMSS logN-logS in numerical form. G.C. Perola, F. La Franca and A. Comastri are thanked for useful discussion. M. Perri acknowledges financial support from a Telespazio research fellowship. Part of the software used in this work is based on the NASA/HEASARC FTOOLS and XANADU packages. This research has made use of the following on-line services: the ASI/BeppoSAX SDC Database and Archive System; the NASA/IPAC National Extragalactic Database, NED; the SIMBAD astronomical database, and the NASA Astrophysics Data System, ADS.

References

Angelini L., Park S., White N.E., P. Giommi, 2000, BAAS 53, 10
Akiyama M., Ohta K., Yamada T., et al., 2000, ApJ, in press astro-ph/0001289
Avni Y., Bachall J.N., 1980, ApJ, 235, 694
Boyle B.J., Jones L.R., Shanks T. 1991, MNRAS 251, 482
Boyle B.J., Shanks T., Georgantopoulos I., Stewart G.C., Griffiths R.E., 1994, MNRAS 271, 639
Boyle B.J., Georgantopoulos I., Blair A.J., et al., 1998, MNRAS 296, 1
Brandt W.N., Hornschemeier A.E., Schnider D.P., et al., 2000, AJ, in press astro-ph/0002121
Boella G., Butler R.C., Perola G.C. et al., 1997a, A&AS 122, 299
Boella G., Chiapetti L., Conti G., et al., 1997b, A&AS 122, 327
Boldt E.A., Desai U.D., Holt S.S., 1969, ApJ 156, 427
Brandt W.N., Horneschemeier A.E., Schneider D.P., et al., 2000, AJ 119, 2349
Burbidge E.M., 1995, A&A 298, L1
Butcher J.A., Stewart G.C., Warwick R.S., et al., 1997, MNRAS 291, 437
Cagnoni I., Della Ceca R., Maccacaro T., 1998, ApJ 493, 54
Ciliegi P., Elvis M., Wilkes B.J., et al., 1995, MNRAS 277, 1463
Comastri A., Setti G., Zamorani G., Hasinger G. 1995, A&A 296,1
Comastri A., 1999, Proceedings of the conference X-ray Astronomy 1999, Bologna, in press
Condon J.J., Cotton W.D., Griesen E.W., et al., 1998, AJ 115, 1693
Della Ceca R., Castelli G., Braito V., 1999a, ApJ 524, 674
Della Ceca R., Braito V., Cagnoni I, and Maccacaro T., 1999b, Proceedings of the conference X-ray Astronomy 1999, Bologna, in press, astro-ph/9912016
Della Ceca R., Maccacaro T., Rosati P., Braito, 2000, A&A 355, 121
Dickey J.M., Lockman F.J., 1990, ARA&A 28, 215
Fabian A.C., 1999, MNRAS 308, L39
Fiore F., La Franca F., Giommi P., et al., 1999, MNRAS 306, L55
Fiore F., La Franca F., Giommi P., et al., 2000a, MNRAS, in press
Fiore F., La Franca F., Vignalo C., et al., 2000b, NewA 5, 143
Garmire G.P., Nousek J.A., Apparao K.M.V., et al., 1992, ApJ 399, 649
Gendreau K.C., Barcons X., Fabian A.C., 1998, MNRAS 297, 41
Georgantopoulos I., Stewart G.C., Blair A.J.,et al., 1997, MNRAS 291, 203
Giacconi R., Bechthold J., Branduardi G., et al., 1979, ApJ 234, L1
Gilli R., Risaliti G., Salvati M., 1999, A&A 347, 424
Giommi P., Tagliaferri G., Beuermann K., et al., 1991, ApJ 378, 77
Giommi P., Fiore F., 1997, Proc. of 5th International Workshop on Data Analysis in Astronomy, Erice
Giommi P., Fiore F., Ricci D., et al., 1998, Nucl. Phys. B, 69/1–3, 591
Giommi P., Menna M.T., Padovani P., 1999b, MNRAS 310, 465
Giommi P., Fiore F., Perri M., 1999a, Astro. Lett. and Communications 39, 173
Gorosabel J., Castro-Tirado A.J., Wolf C., 1998, A&A 339, 719
Greiner J., Hagen H.-J., Heines A., 1996, IAUC 6487
Griffith M.R., Wright A.E., 1993, AJ 105, 1666
Hasinger G., Burg R., Giacconi R., et al., 1993, A&A 275, 1
Hasinger G., Burg R., Giacconi R., et al., 1998, A&A 329, 482
Hewett J.N., Chen G.H., Messier M.D., 1995, AJ 109, 1498
Hewitt A., Burbidge G., 1993, ApJS 87, 451
Inoue H., Kii T., Ogasaka Y., Takahashi T., Ueda Y., 1996 In: Zimmermann H.U., Trümper J., Yorke H. (eds.) Pro. Röntgenstrahlung from the Universe. MPE Report 263, p. 323
Jager R., Mels W.A., Brinkman A.C., et al., 1997, A&AS 125, 557
Kulkarni S.R., Metzger M.R., Frail D.A., et al., 1997, IAUC 6559
La Franca, et al., 2000, in preparation
Lehmann I., Hasinger G., Schmidt M., et al., 2000, A&A 354, 35
Madau P., Ghisellini G., Fabian A.C., 1994, MNRAS 270, L17
Maccacaro T., Della Ceca R., Gioia I.M., et al., 1991, ApJ 374, 117
Marziani P., Sulentic J.W., Dultzin-Hacyan D., et al., 1996, ApJS 104, 37
Marshall F.E., Boldt E.A., Holt S.S., et al., 1980, ApJ 235, 4
McHardy I.M., Jones L.R., Merrifield M.R., et al., 1998, MNRAS 295, 641
Miyaji T., Hasinger G., Schmidt M., 2000, A&A 353, 25
Monnet D.G., 1998, BAAS meeting 193, 120.03
Mushotsky R.F., Cowie L.L., Barger A.J., Arnaud K.A., 2000, Nat 404
Murdoch H.S., Crawford D.F., Jauncey D.L., 1973 ApJ 183, 1
Padovani P., Giommi P., 1995, ApJ 444, 567
Page M.J., Carrera F.J., Hasinger G., et al., 1996, MNRAS 281, 579
Perlman E.S., Padovani P., Giommi P., et al., 1998, AJ 115, 1253
Perri M., Giommi P., 2000, A&A in press
Puchnarewicz E.M., Mason K.O., Carrera F.J., et al., 1997, MNRAS 291, 177
Sacco B., 1999, *Beppo*SAX EIWG meeting report, June 1999.
Schwartz D.A., Murray S.S., Gursky, 1976, ApJ 204, 315
Schmidt M., 1968, ApJ 151, 393
Schmidt M., Hasinger G., Gunn J., et al., 1998, A&A 329,495
Setti G., Woltjer L., 1989, A&A 224, L21
Seward F., Chodil G., Mark H., Swift C., Toor A., 1967, ApJ 150, 845
Stocke J.T., Morris S.L., Gioia I.M., et al., 1991, ApJS 76, 813
Ueda Y., Takahashi T., Inoue H. et al., 1998, Nat 391, 866
Ueda Y., 2000, Astrophysical Letters and Communications, in press, astro-ph/9912084
Vecchi A., Molendi S., Guainazzi M., Parmar A.N., Fiore F., 1999, A&A 349, L73
Vikhlinin A., McNamara B.R., Forman W., et al., 1998, ApJ 502, 558
Voges W., Aschenbach B., Boller T., et al., 2000, IAUC 7432
Warren S.J., Hewett P.C., Osmer P.S., 1991, ApJS 76, 23
White N.E., Giommi P., Angelini L., 1994, IAUC 6100
Wolter A., Gioia I.M., Maccacaro T., Morris S.L., Stocke J.T., 1991, ApJ 369, 314
Zamorani G., Mignoli M., Hasinger G., et al., 1999, A&A 346, 731